CROATICA CHEMICA ACTA CCACAA 63 (3) 401—415 (1990)

CCA-1947

YU ISSN 0011-1643
UDC 541.183
Conference Paper (Invited)

Kinetics and Mechanisms of Photoelectrochemical Reactions at Semiconductor Electrodes*

Laurence M. Peter

Department of Chemistry
The University, Southampton SO9 5NH
Great Britain

Received May 4, 1990

Some kinetic aspects of the photocurrent response of semiconductor electrodes are considered. Particular attention is given to surface recombination, which reduces the photocurrent conversion efficiency, and to photocurrent multiplication, which leads to quantum efficiencies greater than unity. The advantages of non steady-state photocurrent measurements are considered, and it is shown that the coupling of electron and hole fluxes *via* the surface leads to a characteristic time or frequency dependence of the photocurrent conversion efficiency. The principle of intensity modulated photocurrent spectroscopy (IMPS) is described, and its application is illustrated with several examples, including the reduction of oxygen at p-GaAs and the photooxidation of Si in NH_4F. It is shown that frequency response analysis offers unique insights into complex photoelectrode processes of this kind.

INTRODUCTION

The kinetics of electrochemical reactions at metal electrodes have been studied for many years by a wide range of experimental techniques. Most of these methods rely on the fact that it is possible to change the activation barrier, and hence the rate constants, for an electron transfer reaction because the potential drop is located entirely at the metal/solution interface. Different perturbation profiles are used, *e. g.* potential step, linear sweep, sinusoidal potential modulation and so on, and the response is analysed to give values of the standard first order heterogeneous rate constant. It is assumed that the surface concentration of electrons is constant, since the metal simply provides a source or sink for electrons which are transferred at energies close to E_F, the Fermi energy.

The kinetics of reactions at semiconductor electrodes differ in several respects. Firstly, the potential drop is usually located largely in the solid, so that the activation barrier for electron transfer is almost independent of electrode potential. Secondly, electron transfer may involve either majority

* Based on an invited lecture presented at the *8th »Ruđer Bošković« Institute's International Summer Conference on the Chemistry of Solid/Liquid Interfaces* Red Island, Rovinj, Croatia, Yugoslavia, June 22 — Juli 1, 1989.

carriers (*e. g.* electrons if the material is n-type) or minority carriers (*i. e.* holes in the n-type case). Electron transfer takes place from the conduction or valence bands rather than at energies close to E_F, which is located in the bandgap. In the dark, the the surface density of majority carriers is strongly potential dependent. This potential dependence affects the rate of electrode reactions, but it is important to realise that it is the carrier density and not the electron transfer rate constant that is responsible. As a consequence, a second order heterogeneous rate constant must be used to describe semicondur electrode reactions. Semiconductor electrodes are particularly interesting since the equilibrium can be perturbed by illumination, which leads to photocurrents due to photoexcited minority carriers. The purpose of this paper is to examine some kinetic aspects of photoelectrode processes and to show how they can be studied experimentally.

STEADY-STATE PHOTOCURRENTS

Electron transfer reactions at illuminated semiconductor electrodes are determined principally by the behaviour of photoexcited minority carriers, and in the simplest case, the photocurrent will be determined entirely by their collection and transport to the interface. Unfortunately, the amount of useful information available under these conditions is rather limited. If all the collected minority carriers are consumed in an interfacial electron transfer reaction, the photocurrent is given by the Gartner equation[1,2]

$$j_{photo} = I_o\,[1 + \exp\,(-\alpha W)/(1 + \alpha L)] \qquad (1)$$

where α is the absorption coefficient, W is the width of the space charge region and L is the diffusion length of minority carriers. W depends on the potential difference, $\Delta\Phi$, across the semiconductor, and on the relative permittivity ε and the doping density N;

$$W = (2\Delta\Phi\varepsilon\varepsilon_o/qN)^{1/2} \qquad (2)$$

Eqn 1 can be used to analyse photocurrent-voltage curves to give values of L and α,[3,4] but it contains no information about interfacial charge transfer since the photocurrent is entirely determined by the generation and collection of minority carriers in the solid. In practice, the measured photocurrent is usually smaller than predicted by the Gartner equation, particularly close to the flat band potential. The decrease in photocurrent is due to the recombination of electrons and holes *via* bulk or surface energy levels. The most important levels are so-called 'surface states' which can be populated by charge transfer from the solid and electrolyte phases. Their occupation can be derived by kinetic or statistical arguments,[5] but their physical and chemical identity is less easy to establish. Several theoretical models have been discussed in the literature which assess the influence of surface recombination on photocurrent-voltage curves,[2,5] but they are generally of limited usefulness since several different mechanisms may give rise to broadly similar steady state behaviour. Non steady-state methods promise to be key elements in a fresh approach to semiconductor photoelectrochemistry, and so most of this paper is devoted to discussing them. Another promising development which lies outside the scope of this paper is the application of *in-situ* spectroscopy to study the surfaces of semiconductor electrodes.[6,7] Rapid progress has been

made in the application of this approach to metal electrodes, but so far very little work of this kind has been carried out on semiconductor electrodes.

NON-STEADY STATE PHOTOCURRENTS

The importance of transient methods in electrochemistry is well known. Transient perturbation of a photoelectrode process can be achieved at constant potential by controlling the incident light. A square pulse of light, for example, produces a corresponding flux of photogenerated minority carriers, so that the method is analagous to the galvanostatic technique used to study electrode reactions at metals.

An ideal semiconductor/electrode junction should give a simple square response to stepped illumination, but transient relaxation phenomena are often observed in real systems when the illumination is switched on or off. These effects are particularly evident at potentials close to flat band. An example of this behaviour is shown in Figure 1a for p-GaP in acid solution. In this particular case, it has been shown that protons incorporated into the first few atomic layers of the GaP lattice act as surface recombination sites, trapping first photogenerated electrons and then holes.[8] The transient current of opposite sign observed when the illumination is interrupted arises from holes moving from the bulk of the semiconductor to the surface to recombine with electrons trapped on the surface hydrogen states. This process can be described by the simple reaction scheme

$$h\nu \longrightarrow h + e \tag{3a}$$

$$H^+_{lattice} + e \longrightarrow H_{lattice} \tag{3b}$$

$$H_{lattice} + h \longrightarrow H^+_{lattice} \tag{3c}$$

When the light is switched on, electrons flow into the surface region where some of them are captured by H^+ states (reaction 3b), perturbing the equilibrium H/H^+ ratio. The build up of H states leads in turn to an excess hole flux as the velocity of reaction 3c increases, and the photocurrent decays exponentially towards the steady state at a rate that is determined by the velocity of hole capture by H. The relaxation rate is found to depend strongly on electrode potential as shown in Figure 1b. Eqn 3 is typical of the kind of reaction scheme which has to be considered when formulating the non steady state response of semiconductor electrodes. In order to generalise it, it is necessary to include the possibility that a minority carrier trapped at a surface state may react subsequently with a solution redox species.[8-10]

The rate of reaction 3c is potential dependent since the it is first order in the concentration of holes (majority carriers) at the surface, which varies exponentially with band bending under depletion conditions. In the Boltzmann limit, the surface concentration of electrons in an p-type semiconductor is given by

$$P_{surf} = P_{bulk} \cdot \exp(-q\Delta\Phi/kT) \tag{4}$$

so that the rate of eqn 3c is expected to exhibit a 'Nernstian' potential dependence. In fact, as Figure 1b shows, the decay rate varies less rapidly than

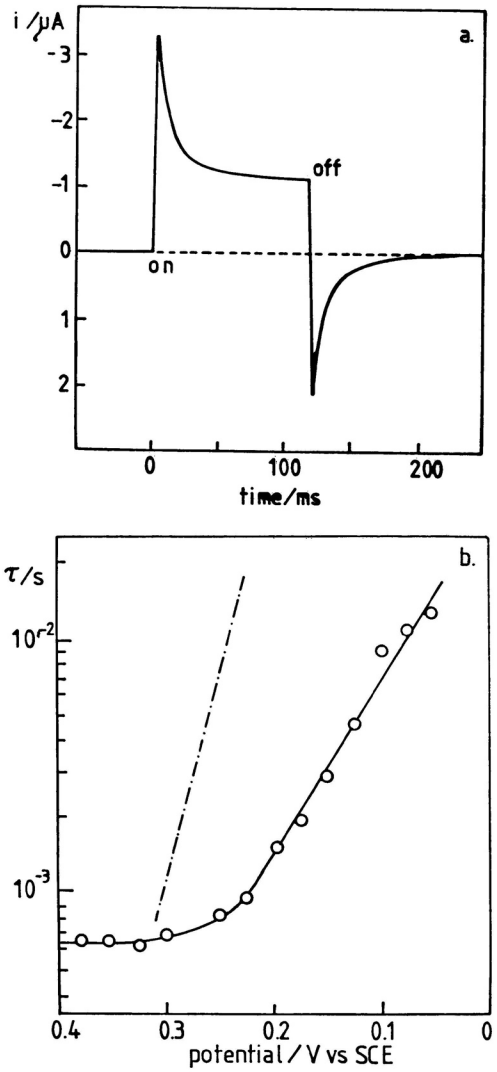

Figure 1. (a) Photocurrent transient for p-GaP in 0.5 mol dm^{-3} H_2SO_4 recorded close to the flatband potential showing relaxation and overshoot due to recombination *via* hydrogen 'near surface states' (eqn 3).

(b) Potential dependence of the relaxation lifetime determined from the exponential decay of photocurrent transients measured at p-GaP. The ideal 'Nernstian' response is shown as a broken line.

expected, and this probably indicates that a substantial fraction of the variation in electrode potential appears across the electrical double layer as the result of charge storage by surface states.

The overall response to different illumination profiles (pulse, step, sinusoidal modulation) can be derived readily by Laplace transform methods,

and full details have been given elsewhere.[8-11] The experimental photocurrent response is also shaped by the transfer function of the electrochemical cell, which is determined by the parallel combination of the space charge capacitance, C_{sc}, and the solution resistance, R_{sol}. In the present case, where the response in the time domain is of interest, we may write the photocurrent as

$$j_{photo}\ (t) = j_{hole}\ (t) + j_{electron}\ (t) \tag{5}$$

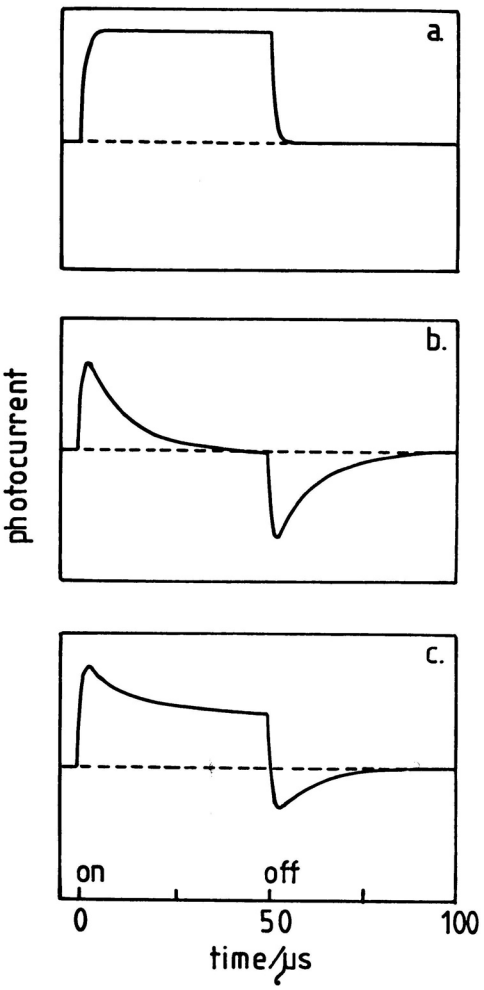

Figure 2. Photocurrent response calculated for the scheme in eqn. 3 showing the effects of recombination and of the time constant $R_{sol}\,C_{sc}$ ($= 10^{-5}$ s).

(a) No surface recombination.
(b) Complete recombination
(c) Partial recombination

Figure 2 compares the transient photocurrent responses to chopped illumination that are expected for three cases: a) no recombination, b) complete recombination and c) partial recombination. It can be seen that the risetime of the photocurrent is determined simply by the $R_{sol}C_{sc}$ time constant, whereas the time constant associated with the decay and overshoot is determined by the rate of majority carrier capture by the surface state (reaction 3c).

INTENSITY MODULATED PHOTOCURRENT SPECTROSCOPY (IMPS)

It is clear that the transient photocurrent response in Figure 1a must have its analogue in the frequency domain. This is the basis of intensity modulated photocurrent spectroscopy (IMPS). The method involves sinusoidal modulation of the illumination intensity using the apparatus shown in Figure 3.[10,11] The intensity of the incident laser beam is modulated by an acousto-optic modulator driven by the d. c. biased output from a frequency response analyser. The depth of modulation can be varied from zero up to about 0.9. Measurements are made under potentiostatic control using a fast potentiostat built from operational amplifiers. Particular attention must be paid to cell design in order to be able to carry out measurements up to 50 kHz. The complex ratio of the a. c. component of the photocurrent to the incident modulated light flux is obtained by deriving a reference signal from a fast photodiode which samples the laser beam. It is worth stressing that IMPS is not equivalent to ac impedance. It measures a complex ratio of two currents, *i. e.* a complex gain, which is a dimensionless quantity.

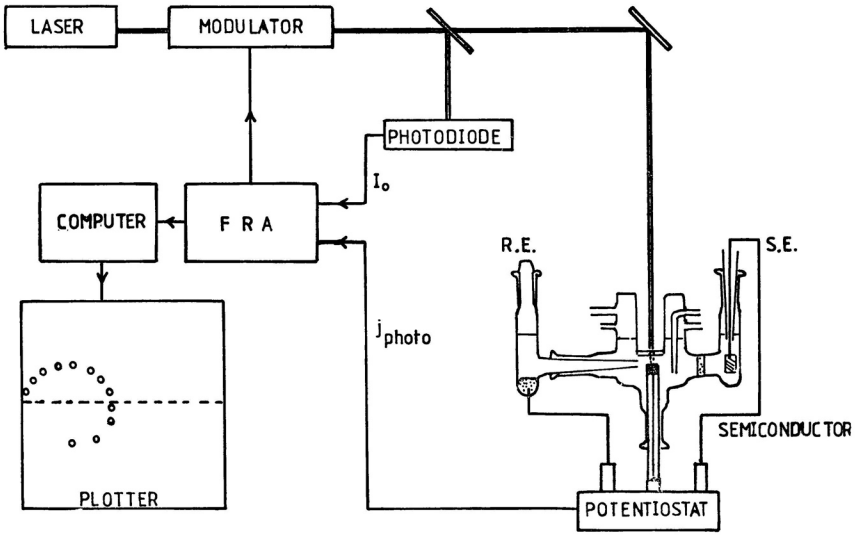

Figure 3. Experimental arrangement for intensity modulated photocurrent spectroscopy (IMPS).

The modulated photocurrent response can be written as a frequency dependent complex gain

$$j_{\text{photo}}(\omega)/g(\omega) = \text{Real}\,(j_{\text{photo}}(\omega)) + j\ \text{Imag}\,(j_{\text{photo}}(\omega)) \quad (6)$$

Here $g(\omega)$ represents the *a. c.* component of the interfacial minority carrier flux corresponding to the Gartner equation (eqn 1). The normalization is convenient since the ratio in eqn 6 will be unity in the absence of surface recombination provided that the measurement is made at sufficiently low frequencies that attenuation by the cell ($R_{\text{sol}}C_{\text{sc}}$) is negligible. More generally, however, the magnitude of the complex gain will be less than zero as a result of attenuation associated with the interfacial and cell transfer functions.

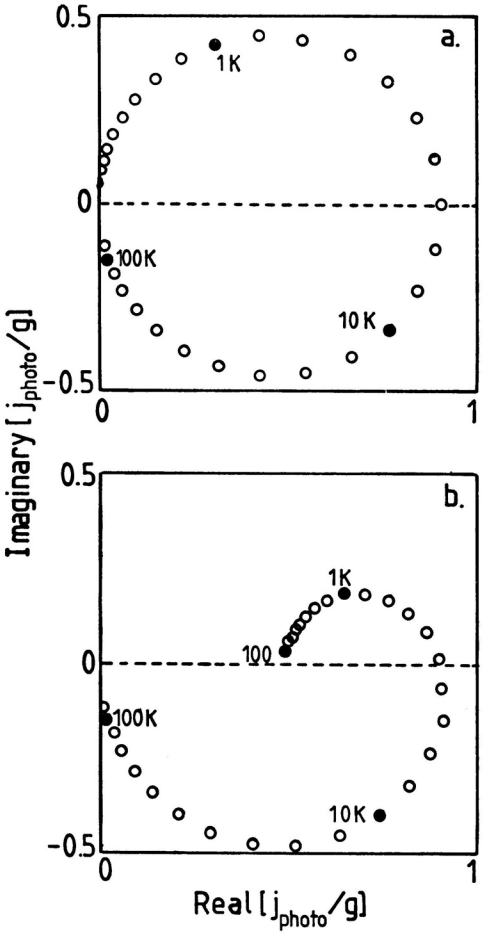

Figure 4. Theoretical IMPS plots calculated for (a) complete recombination (b) partial recombination. Note that the frequency of the maximum is determined by the rate of majority carrier capture. The fre.uency of the minimum is determined by R_{sol} C_{sc}.

The general trends in the IMPS response are illustrated by two examples in Figure 4. If recombination is complete, the response extends from the first into the fourth quadrant of the complex plane (Figure 4a). Both the low

and high frequency intercepts are located at the origin. Interestingly, this means that the steady state photocurrent is essentially zero, whereas the quantum efficiency of the periodic photocurrent approaches unity! The response in the upper quadrant is determined by the kinetics of surface recombination, and the response in the lower quadrant depends on the time constant $R_{sol}C_{sc}$. If indirect charge transfer *via* surface states is negligible, the radial frequency of the maximum in the upper quadrant is equal to the pseudo first rate constant for majority carrier capture by the surface states. The more general case of partial recombination is shown in Figure 4b. In this example, only half of the minority carriers are captured by surface states, so that the low frequency intercept in the first quadrant is located at 0.5, *i. e.* the quantum efficiency in the steady state is 0.5. The response again moves from the first into the fourth quadrant as the frequency is increased as a result of attenuation of the photocurrent by $R_{sol}C_{sc}$. In general, it should be possible to separate the time constants associated with recombination and external attenuation provided that they differ by at least than one order of magnitude. Finally, it should be noted that diameter of the upper semicircle decreases and the low frequency intercept tends towards unity as recombination effects become smaller with increasing band bending.

The IMPS technique has been applied to the study of the photoelectrochemical behaviour of n-GaAs in alkaline solutions.[10,12] Figure 5a is a photocurrent-voltage curve measured for an n-type GaAs electrode in alkaline selenide solution. A conventional lock-in technique was used with chopped illumination to record this curve, which shows evidence of hysteresis and of recombination close to the flatband potential. The dangers inherent in using lock-in methods to measure 'steady state' photocurrent voltage curves are demonstrated by Figure 5b which illustrates the relationship between the photocurrent responses in the time and frequency domains (IMPS) at three different potentials. The results show clearly the transition from the recom-

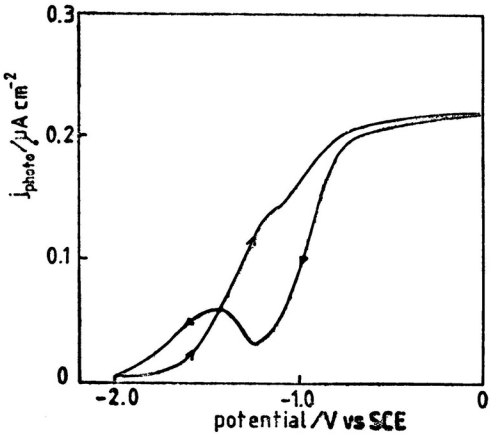

Figure 5. (a) Photocurrent potential plot for n-GaAs in 0.1 mol dm^{-3} KOH, 1.4×10^{-3} mol dm^{-3} K_2Se measured at an incident light slux of 4×10^{15} cm^{-2} (633 nm). Note that the photocurrent onset is displaced away from the flatband potential (—2.1 V) and that the response shows hysteresis between the forward and reverse sweeps due to changes in surface composition.

Fig. 5. to be continued

Fig. 5. continued

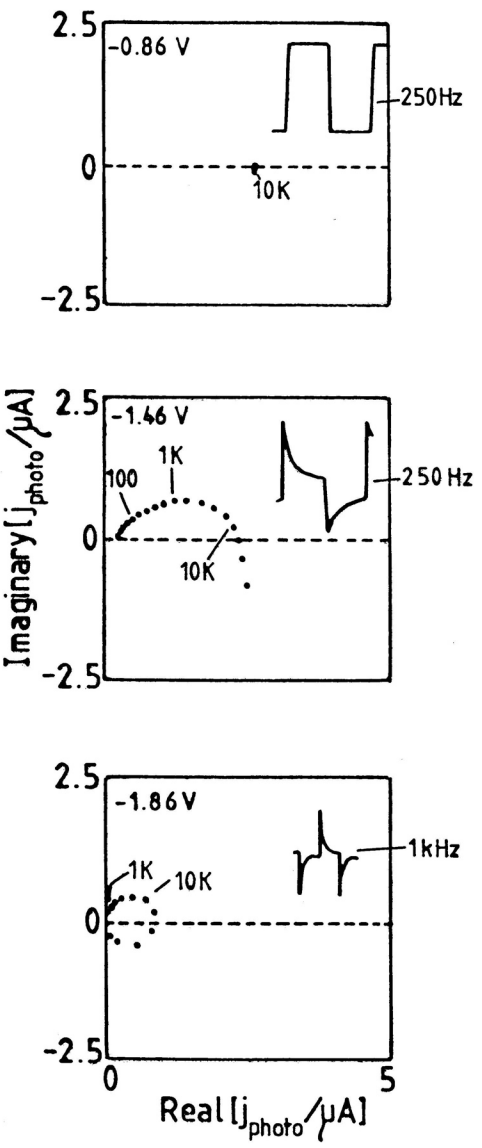

(b) Comparison of transient photocurrent and IMPS response of n-GaAs under the same conditions as (a). Note the transition from recombination free behaviour in the plateau photocurrent region (—0.86 V) to essentially complete recombination close to the flatband potential.

bination-free situation to almost complete recombination close to the flatband potential. A detailed analysis of the potential dependence of the recombination rate has been performed using IMPS, and the results show that the composition of the GaAs/solution interface and hence the interfacial dipole potential changes with electrode potential. The effect of adsorbing ruthenium species

on the surface of n-GaAs has been investigated. The IMPS data show clearly that the interface has been stabilised and that the behaviour of the photoanode approaches the ideal limit more closely. Further discussion of these results has been given elsewhere.[10]

PHOTOCURRENT DOUBLING AND QUADRUPLING

Under normal circumstances, the photocurrent quantum efficiency of a photoelectrochemical cell is expected to be less than or equal to unity. There are, however, interesting cases where the quantum efficiency (electrons per absorbed photon) can exceed unity. An example of this effect is the reduction of oxygen to hygrogen peroxide at illuminated p-GaP[13] an p-GaAs.[14-16] Photocurrent-potential which demonstrates the 'current doubling effect' are shown in Figure 6a. The quantum efficiency for the reduction process approaches 2 at low light intensities since the $HO_2\cdot$ intermediate injects a hole into the valence band;

$$h\nu \longrightarrow h + e \tag{7a}$$

$$O_2 + H^+ + e \longrightarrow HO_2\cdot \tag{7b}$$

$$HO_2\cdot + H^+ \longrightarrow H_2O_2 + h \tag{7c}$$

Reaction 7c competes with photoelectron capture by $HO_2\cdot$ (eqn 7b), so that current doubling is only observed when the illumination level is sufficiently low that hole injection injection predominates. The injection of electrons introduces an additional relaxation process into the periodic photocurrent response so that the measured photocurrent is made up of three separate fluxes;

$$j_{photo} = j_{electron} + j_{hole} + j_{injection} \tag{8}$$

Deconvolution of these components is impossible in the steady-state, but under periodic illumination, the different frequency response associated with each component allows them to be separated. A detailed theoretical analysis which includes the effects of surface recombination has been presented elsewhere.[16] The main features of the IMPS solution are summarised in Figure 6b. In the absence of appreciable surface recombination (*i. e.* in the region of the photocurrent plateau in Figure 6a), the IMPS response is expected to be located in the fourth quadrant of the complex plane. The low frequency intercept occurs at 2 since the injection of holes follows the driving function without attenuation. As the frequency is increased, however, the periodic component associated with hole injection is attenuated and the IMPS plot traces out a semicircle which intercepts the real axis at unity at high frequencies (the effects of the $R_{sol}C_{sc}$ time constant have been omitted for clarity). The frequency of the minimum of the semicircle is simply the inverse of the rate constant for reaction 7c.

Figure 6 also shows the predicted effects of surface recombination. As the band-bending is reduced, the low frequency part of the IMPS response moves into the upper plane, and the low frequency intercept falls below 2. It is worth noting that the photocurrent doubling effect may not be visible in the steady state photocurrent under these conditions, whereas it can be detected readily in the IMPS response.

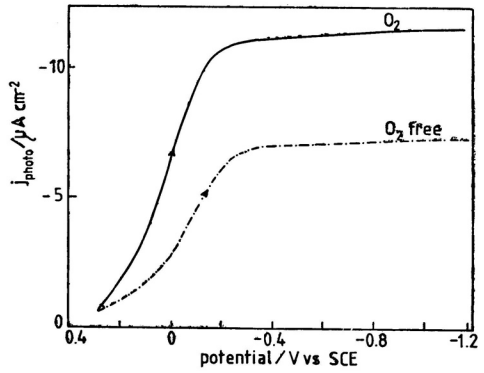

Figure 6. (a) Photocurrent potential plots for p-GaAs in 0.5 mol dm^{-3} H_2SO_4 showing the photocurrent doubling effect in the presence of oxygen. Illumination 632.8 nm, 1.7×10^{-5} W cm^{-2}.

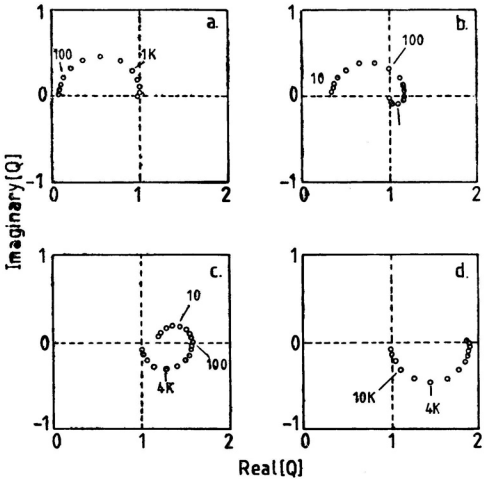

(b) Theoretical IMPS plots calculated for current doubling. The effects of recombination are also taken into account, and the plots show the changes in the IMPS signature that are predicted to occur as the band bending is increased from a to d. Surface state density 10^{12} cm^{-2}. The surface state is assumed to be situated 0.3 eV above the bulk Fermi energy.

Fig. 6. to be continued

Figure 6c shows experimental IMPS plots for p-GaAs in oxygen saturated acid solution which confirm the predicted transition between the photocurrent doubling and recombination limits. Further details are given in ref. 16. The pseudo first-order rate constant for the injection of holes was found to be 2.5×10^4 s^{-1},[16] which corresponds to an activation energy for hole injection of around 0.4 eV.

A second example of photocurrent multiplication is observed during the photoanodic dissolution of n-Si in ammonium fluoride solutions. Here quantum efficiencies approaching 4 have been observed at low light intensities,[17] indicating that steps in the dissolution mechanism involve electron injection. The following simplified reaction scheme suffices for the kinetic analysis.

Fig. 6. continued

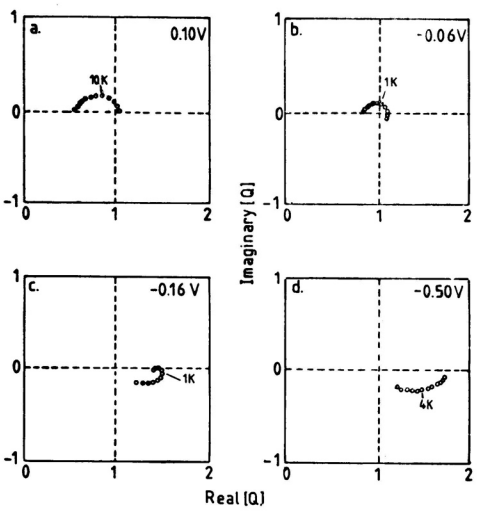

(c) Experimental IMPS plots for p-GaAs in oxygen saturated 0.1 mol dm^{-3} $HClO_4$. Note the transition from current doubling behaviour to recombination control. The rate constant for hole injection by $HO_2\cdot$ is obtained from the frequency at which the minimum in the lower complex plane occurs.

$$h\nu \longrightarrow h + e \tag{9a}$$

$$Si\ (0) + h \xrightarrow{k_o} Si(I) \tag{9b}$$

$$Si\ (I) \xrightarrow{k_a} Si(II) + e \tag{9c}$$

$$Si\ (II) \xrightarrow{k_b} Si(III) + e \tag{9d}$$

$$Si\ (III) \xrightarrow{k_c} Si(IV) + e \tag{9e}$$

Here Si(I) — Si(III) represent the nominal valence states of surface intermediates, whereas Si(IV) is the final product, SiF_6^{2-}. As in the previous example, majority carrier injection competes with minority carrier capture so that current multiplication is only observed at low intensities where the intermediates react predominantly *via* the injection route rather than by capturing further photogenerated holes.

Each electron injection step gives rise to a corresponding component, j_{inj}, in the total photocurrent:

$$j_{photo} = j_{hole} + j_{inj}^{I} + j_{inj}^{II} + j_{inj}^{III} \tag{10}$$

Although these fluxes cannot be deconvoluted in the steady-state, they can be distinguished, at least in principle, in the time or frequency domains since each injection step is characterised by a different rate constant.

The solution of this kinetic scheme for the case of periodic illumination[18] predicts the IMPS responses shown in Figure 7a. The theory shows that one, two or three semicircles may be observed, depending on the relative values of the rate constants for the three electron injection steps. Three semicircles are expected only in the special case where $k_a > k_b > k_c$.

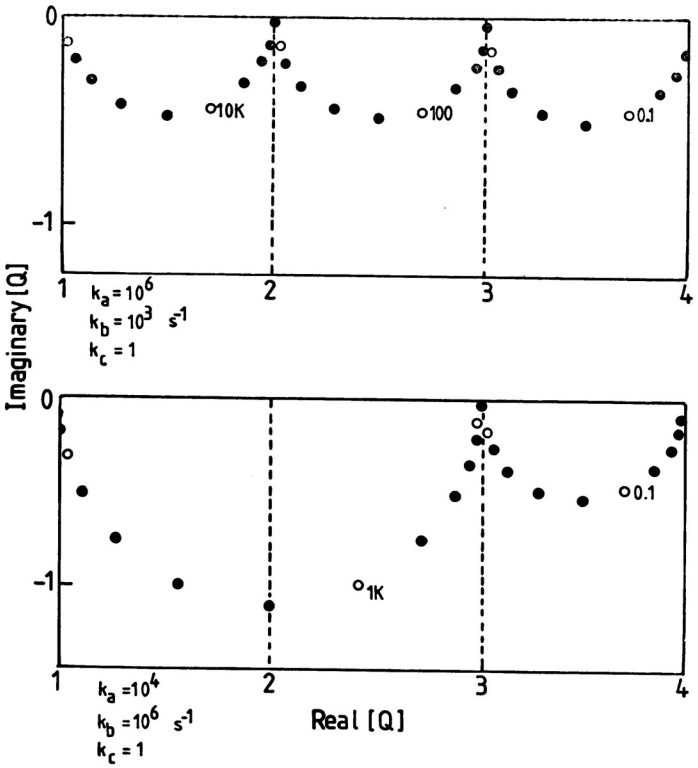

Figure 7. (a) Examples of the theoretical IMPS plots for photocurrent quadrupling showing the time constants associated with the electron injection steps. In the first case, the rate constants for electron injection decrease in the order $k_a > k_b > k_c$ so that three semicircles are observed in the fourth quadrant. In the second case, the order is $k_b > k_a > k_c$, and the first two injection steps give rise to a semicircle with double the radius. Note that the low frequency intercept at $Q = 4$ corresponds to photocurrent quadrupling, whereas the low frequency intercept is located at $Q = 1$ (the influence of $R_{sol}\,C_{sc}$ has been neglected).

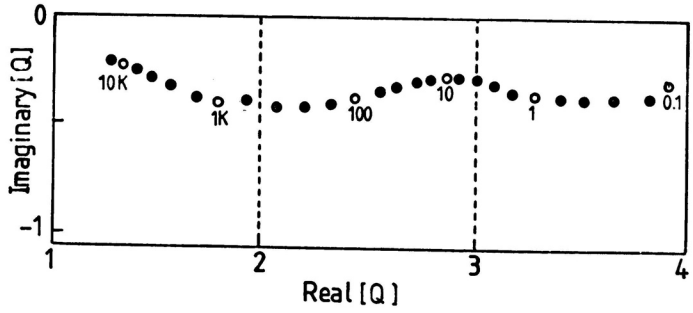

(b) Experimental IMPS plots obtained for n-Si in 6.5 mol dr^{-3} NH_4F (pH 5.4) in the saturation photocurrent region. The data have been fitted for $k_a = 2 \times 10^4$ s^{-1}, $k_b = 500$ s^{-1} and $k_c = 0.5$ s^{-1} and a standard deviation of 1.5 kT in the activation energies for the electron injection steps.

The experimental IMPS result presented in Figure 7b displays the main features predicted by the theory, although the semicircles are flattened, probably because electron injection occurs at different surface sites. The frequency response has been fitted successfully by assuming a normal distribution of activation energies for the injection step.[18] The rate constants for the electron injection steps are rather low in this case, indicating that they involve thermally activated bond breaking. Estimates of the energies involved lie in the region 0.3 to 0.4 eV. A full analysis of this interesting system is given elsewhere.[19]

CONCLUSION

This brief survey of kinetic aspects of semiconductor photoelectrochemistry has demonstrated the importance of non-steady state methods such as IMPS which allow deconvolution of the contributions to the photocurrent of minority, majority and injected carriers. The dependence of the rates of surface processes on potential, solution composition and surface orientation and preparation can now be studied in detail, opening a new area of dynamic semiconductor photoelectrochemistry.

Acknowledgments. — Financial support for this work was provided by the Science and Engineering Research Council. The author thanks J. G. Li, R. Peat, J. Stumper and H. J. Lewerenz, who have collaborated in this area of research, and the organisers of the *VIII International Conference 'Chemistry of Solid/Liquid Interfaces'* for their invitation to present this paper.

REFERENCES

1. W. W. Gartner, *Phys. Rev.* **116** (1954) 84.
2. L. M. Peter in Specialist Periodical Report *'Electrochemistry'*, Vol. 9, p. 66. Editor D. Pletcher. Royal Society of Chemistry, London 1984.
3. J. Li, R. Peat, and L. M. Peter, *J. Electroanal. Chem.* **165** (1984) 42.
4. R. Peat and L. M. Peter, *Appl. Phys. Lett.* **51** (1987) 328.
5. L. M. Peter, J. Li, and R. Peat, *J. Electroanal. Chem.* **165** (1984) 29.
6. L. M. Peter, D. J. Blackwood, and S. Pons, *Phys Rev. Lett.* **62** (1989) 308.
7. A. Venkateswara Rao and J. N. Chazalviel, *J. Electrochem. Soc.* **34** (1987) 2777.
8. L. M. Peter and J. Li, *J. Electroanal. Chem.* **193** (1985) 27.
9. L. M. Peter in *Photocatalysis and the Environment.* NATO ASI series p. 243. Editor M. Schiavello. Kluwer, Dordrecht 1988.
10. R. Peat and L. M. Peter, *Ber. Bunsenges. Phys. Chem.* **91** (1987) 381.
11. L. M. Peter, J. Li, R. Peat, H. J. Lewerenz, and J. Stumper, *Electrochim. Acta* (in press).
12. J. Li and L. M. Peter, *J. Electroanal. Chem.* **199** (1986) 1.
13. J. Li and L. M. Peter, *J. Electroanal. Chem.* **182** (1985) 399.
14. J. Li, R. Peat, and L. M. Peter, *J. Electroanal. Chem.* **200** (1986) 333.
15. R. Peat and L. M. Peter, *Electrochim. Acta* **31** (1986) 731.
16. R. Peat and L. M. Peter, *J. Electroanal. Chem.* **209** (1986) 307.
17. M. Matsumura and S. R. Morrison, *J. Electroanal. Chem.* **147** (1983) 157.
18. H. J. Lewerenz, J. Stumper, and L. M. Peter, *Phys. Rev., Lett.* **61** (1988) 1989.
19. L. M. Peter, H. J. Lewerenz, and J. Stumper, *J. Electroanal. Chem* (submitted).

SAŽETAK

Kinetika i mehanizmi fotoelektrokemijskih reakcija na poluvodičkim elektrodama

L. M. Peter

U radu se razmatraju kinetički parametri fotostrujnog odgovora poluvodičkih elektroda. Posebna je tema rekombinacija na površini, koja smanjuje djelotvornost pretvorbe fotostruje, te multiplikacija fotostruje koja vodi prema kvantnoj djelotvornosti većoj od jedinice. Metodološki se u radu obrađuju mjerenja fotostruja u nestacionarnom stanju, i pokazuje, da međusobno povezivanje toka elektrona i šupljina preko površine prouzrokuje karakteristične vremenske ili frekventne ovisnosti djelotvornosti konverzije. Opisani su principi intenzitetno modulirane fotostrujne spektroskopije, a njena primjena opisana je na nekoliko primjera s n- i p-GaAs kao fotoelektrodom za redukciju kisika odnosno fotooksidaciju Si u NH_4F. Analiza frekventnog odziva ukazuje se kao tehnika s izrazitim uvidom u kompleksne fotoelektrodne procese.